

# Crystal Structures of PDE4D in Complex with Roliprams

Q. Huai, H. Wang, Y. Sun, H.Y. Kim, Y. Liu, H. Ke

Department of Biochemistry and Biophysics and Lineberger Comprehensive Cancer Center,  
University of North Carolina, Chapel Hill, NC, U.S.A.

## Introduction

Cyclic nucleotide phosphodiesterases (PDEs) are a superfamily of enzymes controlling cellular concentrations of the second messengers cAMP and cGMP [1-3]. To date, 11 families and more than 60 isoforms of PDEs have been reported [1, 4-9]. The molecules of all PDE families contain a conserved catalytic domain. However, each PDE family recognizes a specific substrate and possesses its own selective inhibitors. Thus, the families of PDE4, 7, and 8 prefer to hydrolyze cAMP, while PDE5, 6, and 9 are cGMP specific. PDE1, 2, 3, 10, and 11 take both cAMP and cGMP as their substrates. On the other hand, selective inhibitors against the different PDE families have been widely studied as pharmaceutical agents for treatment of various human diseases [10-14]. For example, the PDE5 inhibitor sildenafil (Viagra) is a drug for male erectile dysfunction. Selective inhibitors of PDE4 form the largest group of inhibitors for any PDE family and have been studied as anti-inflammatory drugs targeting asthma and chronic obstructive pulmonary disease [13-17]. How selective inhibitors with different chemical structures bind to the conserved catalytic pockets of PDEs remains a mystery. Herein, we report on the crystal structures of the catalytic domain of human PDE4D2 in complex with (R)-rolipram or (R,S)-rolipram. These structures reveal the selective binding of roliprams to PDE4 and suggest that the inhibitor selectivity is determined by chemical nature of amino acids.

## Methods and Materials

### Protein Expression and Purification

The cDNA clones of PDE4D2 (BF059733) were purchased from ATCC and subcloned following standard methods. The coding region for amino acids 79-438 of PDE4D2 was subcloned into vector pET15b and expressed in *E. coli strain* BL21. The recombinant PDE4D2 was purified by Ni-NTA affinity column, thrombin cleavage, Q-sepharose, and Superdex 200 columns. A typical purification yielded over 100 mg of PDE4D2 from a 2-L cell culture.

### Crystallization and Data Collection

The crystals of the catalytic domain of PDE4D2 in complex with (R)-rolipram were grown against a well buffer of 0.1 M HEPES (pH 7.5), 20% PEG3350, 30% ethylene glycol, 10% isopropanol, and 5% glycerol at

4°C. It has the space group  $P2_12_12_1$  with cell dimensions of  $a = 99.3$ ,  $b = 112.5$ , and  $c = 160.9$  Å. The diffraction data were collected on beamline X25 at Brookhaven National Laboratory (Table 1). The complex of PDE4D2 catalytic domain with racemic (R,S)-rolipram was crystallized against a well buffer of 0.05 M HEPES (pH 7.5), 20% PEG3350, 25% ethylene glycol, and 10% isopropanol at 4°C. It has the space group  $P2_12_12_1$  with cell dimensions of  $a = 99.8$ ,  $b = 111.5$ , and  $c = 160.0$  Å. The diffraction data were collected on beamline 14-C of the APS (Table 1).

TABLE 1. Statistics on diffraction data and structure refinement of PDE4D inhibitors

Parameter	(R,S)-rolipram	(R)-rolipram
<b>Data collection</b>		
Resolution (Å)	2.0	2.3
Total measurements	677,028	491,376
Unique reflections	89,779	77,976
Completeness (%)	86.7 (69.1) <sup>a</sup>	97.0 (75.6)
Average I/σ	20.0 (3.8)	14.0 (2.8)
Rmerge	0.065 (0.54)	0.053 (0.25)
<b>Structure refinement</b>		
R-factor	0.233	0.224
R-free	0.266	0.260
Resolution (Å)	50-2.0	50-2.3
Reflections	89,775	75,736
RMS deviation for:		
Bond (Å)	0.0061	0.0062
Angle	1.21°	1.19
<sup>a</sup> Numbers in parentheses are for highest-resolution shell.		

### Structure Determination

The crystals of PDE4D2 in complex with roliprams contain a tetramer in the crystallographic asymmetric unit. The structure of PDE4D2-rolipram was solved by the molecular replacement program AMoRe [18], by using the catalytic domain of PDE4B as the initial model [19]. The tetramer of PDE4D-rolipram was optimized by rigid-body refinement of CNS [20]. The electron density map was improved by the density modification package of CCP4 [21]. The atomic model was rebuilt by program O [22] and refined by CNS (Table 1).

## Results and Discussion

### Architecture of PDE4D-Rolipram Structure

Four molecules of the catalytic domain of PDE4D2 with amino acids 79-438 are associated into a tetramer in the crystallographic asymmetric unit (Fig. 1). The monomeric PDE4D2 molecule contains 16 helices and has the same folding as that of PDE4B, except for the random loop of residues 422-434 in PDE4D2 in correspondence to helix H17 in PDE4B [19].

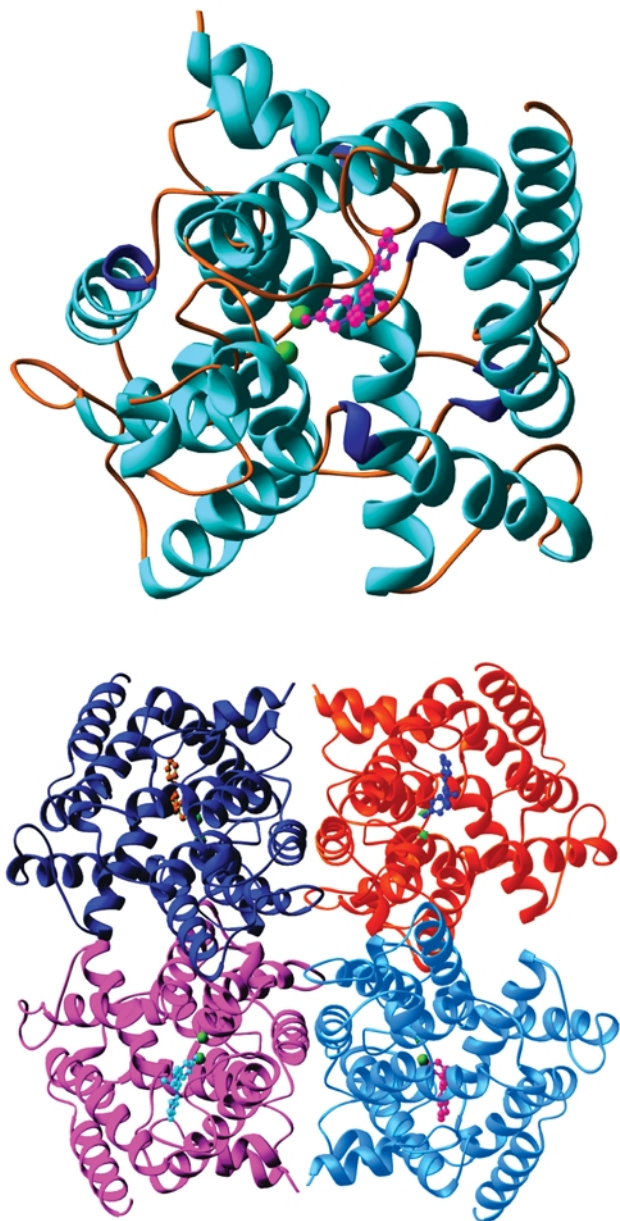


FIG. 1. Ribbon diagram of monomer (top) and tetramer (bottom) of PDE4D2 catalytic domain. Rolipram is shown as the pink balls (top), while two divalent metals are shown as green balls. © 2003 Cell Press, *Structure*, Vol 11, 865-873, July 2003.

### Rolipram Binding

The (R)- and (R,S)-roliprams bind to the active site of PDE4D2 with similar orientations and interact with the same residues (Fig. 2). Roliprams form two hydrogen bonds with the side chain of Gln369 and have numerous hydrophobic interactions with the active site residues. The cyclopentyloxy groups of (R)- and (S)-roliprams sit in a hydrophobic pocket, interacting with residues Ile336, Met337, Phe340, Met357, Ser368, Gln369, and Phe372. The phenylmethoxy rings of (R)- and (S)-roliprams stack over Phe372 and also contact Tyr159, Asn321, Tyr329, Thr333, Ile336, and Gln369 via van der Waals forces. Although the pyrrolidone groups of (R)- and (S)-roliprams have an opposite chirality, they unexpectedly interact with the same residues of PDE4D2. Surprisingly, the pyrrolidone rings, which are anchored in the direction of the metal binding pocket, form no hydrogen bonds with the active site residues or divalent metals but form polar interactions with His160, Met273, Leu319, Phe340, and Phe372.

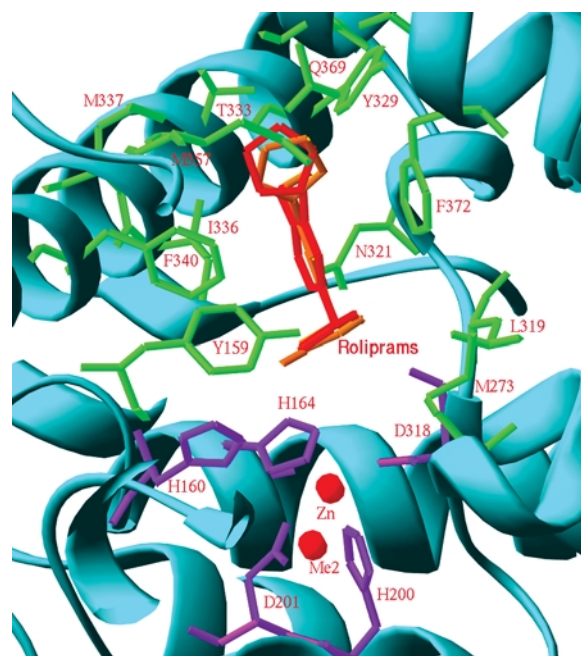


FIG. 2. Binding of (R)- and (S)-roliprams at the catalytic pocket of PDE4D2. Zinc coordinates with His164, His200, Asp201, and Asp318 (purple). The second metal (Me2) is tentatively interpreted as magnesium and binds to Asp318 and a water molecule. © 2003 Cell Press, *Structure*, Vol 11, 865-873, July 2003.

### Implications on Inhibitor Selectivity

The structure-based sequence alignment of the rolipram-binding residues provides clues into inhibitor selectivity (Fig. 3). Gln369 is the only rolipram-binding

residue absolutely conserved in all PDE families. Since hydrogen bonds are major factors for determining the accurate orientation of a ligand, Gln369 and its conformation must play a key role in inhibitor binding and selectivity. Hydrophobic residues Tyr195, Met273, Leu319, Trp332, Ile336, Phe340, Met357, and Phe372 are conservatively substituted in other families of PDE. These residues contribute the hydrophobic interactions to the binding of inhibitors, and their important roles are confirmed by the mutagenesis data [23, 24]. The variation of these residues will determine the size and shape of the binding pockets in different PDE families, thus defining inhibitor selectivity. Asn321, Tyr329, and Ser368 are three residues showing the largest variation across the PDE families (Fig. 3) and must play critical roles in defining inhibitor selectivity. In short, we speculate that the inhibitor selectivity is determined by a combination of different amino acids and subtle conformational changes at the active site of each PDE family.

### Acknowledgments

Use of the APS was supported by the DOE Office of Science, Office of Basic Energy Sciences, under Contract No. W-31-109-ENG-38. Data were collected at beamline 14-C at APS and beamlines X25 and X12C at NSLS. This work was supported in part by the National Institutes of Health (GM59791 to Ke). The coordinates have been deposited in the Protein Data Bank with accession codes 1Q9M and 1OYN. Details on this report can be found in *Structure* [25].

### References

- [1] T.J. Torphy, *Am. J. Respir. Crit. Care* **157**, 351-370 (1998).
- [2] M. Conti and S.L. Jin, *Prog. Nucleic Acid Res. Mol. Biol.* **63**, 1-38 (1999).
- [3] S.H. Soderling and J.A. Beavo, *Curr. Opin. Cell Biol.* **12**, 174-179 (2000).
- [4] M.D. Houslay and G. Milligan, *Trends Biochem. Sci.* **22**, 217-224 (1997).
- [5] J.D. Corbin and S.H. Francis, *J. Biol. Chem.* **274**, 13729-13732 (1999).
- [6] M.D. Housaly and D.R. Adams, *Biochem. J.* **370**, 1-18 (2003).
- [7] V.C. Manganiello, M. Taira, F. Degerman, and P. Belfrage, *Cell. Signalling* **7**, 445-455 (1995).
- [8] C.M. Mehats, C.B. Anderson, M. Filopanti, S.L.C. Jin, and M. Conti, *Endocrinol. Metab.* **13**, 29-35 (2002).
- [9] T. Müller, P. Engels, and J.R. Fozard, *Trends Biochem. Sci.* **17**, 294-298 (1996).
- [10] M.P. Reilly and E.R. Mohler III, *Ann. Pharmacother.* **35**, 48-56 (2001).
- [11] D.P. Rotella, *Nat. Rev. Drug Discov.* **1**, 674-682 (2002).
- [12] M.A. Giembycz, *Monaldi Arch. Chest Dis.* **57**, 48-64 (2002).
- [13] J.E. Souness, D. Aldous, and C. Sargent, *Immunopharmacology* **47**, 127-162 (2000).
- [14] Z. Huang, Y. Ducharme, D. Macdonald, and A. Robichaud, *Curr. Opin. Chem. Biol.* **5**, 432-438 (2001).
- [15] V. D. Piaz and P. Giovannoni, *Eur. J. Med. Chem.* **35**, 463-480 (2000).

	160	164	200	273	318	321	329	332	336	340	357	368	372
pde4d2	YH	H	HD	M	DL	N	Y	WT	IM	F	M	SQ	F
pde4b2b	YH	H	HD	M	DL	N	Y	WT	IM	F	M	SQ	F
pde3a1	YH	H	HD	L	DI	G	H	WT	IV	F	M	LQ	F
pde7a	YH	H	HD	I	DI	N	S	WS	VT	F	L	IQ	F
pde8a	YH	H	HD	M	DV	N	C	WA	IS	Y	V	SQ	F
pde1a3a	YH	H	HD	M	DI	H	H	WT	LM	F	L	SQ	F
pde2a3	YH	H	HD	L	DL	D	T	IA	IY	F	M	LQ	F
pde10a2	YH	H	HD	L	DL	S	T	TA	IY	F	M	GQ	F
pde11a	YH	H	HD	L	DL	A	S	VA	VT	F	I	LQ	W
pde5a1	YH	H	HD	L	DL	A	Q	IA	VA	F	L	MQ	F
pde6a	YH	H	HD	L	DL	A	Q	VA	VA	F	M	LQ	F
pde9a1	FH	H	HD	M	DI	N	A	WV	LL	Y	F	AQ	F
		*	**		*								

FIG. 3. Sequence alignment of the rolipram binding residues among 11 PDE families. The metal binding residues are marked with \*. Most of the rolipram binding residues are conserved but are not conserved identically, implying their key roles in defining inhibitor selectivity. © 2003 Cell Press, *Structure*, Vol 11, 865-873, July 2003.

- [16] M.S. Barnette and D.C. Underwood, *Curr. Opin. Pulm. Med.* **6**, 164-169 (2000).
- [17] G. Sturton and M. Fitzgerald, *Chest* **121**, 192s-196s (2002).
- [18] J. Navaza and P. Saludjian, *Methods Enzymol.* **276**, 581-594 (1997).
- [19] R.X. Xu et al., *Science* **288**, 1822-1825 (2000).
- [20] A.T. Brünger et al., *Acta Crystallogr.* **D54**, 905-921 (1998).
- [21] Collaborative Computational Project, Number 4, *Acta Crystallogr.* **D50**, 760-763 (1994).
- [22] T.A. Jones, J.-Y. Zou, S.W. Cowan, and M. Kjeldgaard, *Acta Crystallogr.* **A47**, 110-119 (1991).
- [23] W. Richter, L. Unciuleac, T. Hermsdorf, T. Kronbach, and D. Dettmer, *Cell. Signalling* **13**, 287-297 (2001).
- [24] J.M. Atienza, D. Susanto, C. Huang, A.S. McCarty, and J. Colicelli, *J. Biol. Chem.* **274**, 4839-4847 (1999).
- [25] Q. Huai, H. Wang, Y. Sun, H.Y. Kim, Y. Liu, and H. Ke, "Three dimensional structures of PDE4D in complex with roliprams and implication on inhibitor selectivity," *Structure* **11**, 865-873 (2003).